Structural transformation and spin-reorientation transition in epitaxial Fe/Cu_3Au(100) ultrathin films

M.-T. Lin,* J. Shen, W. Kuch, H. Jenniches, M. Klaua, C. M. Schneider, and J. Kirschner
Max-Planck-Institut für Mikrostrukturphysik, Weinberg 2, D-06120 Halle, Germany
(Received 5 August 1996)

The magnetic properties, morphology, and crystallographic structure are studied for Fe films on $Cu_3Au(100)$ grown at room and low temperature, using *in situ* magneto-optical Kerr effect, scanning tunneling microscopy, and electron diffraction techniques. At $T=160$ K a spin-reorientation transition from perpendicular to in-plane magnetization occurs in films with Fe coverages starting from a critical thickness of 3.5 and 5.5 ML for room-temperature and low-temperature growth, respectively. Close to the critical thickness we observe an fcc-bcc structural transformation. The spin-reorientation transition is shown to be correlated to this structural change. This correlation may be explained by a drastic reduction of the perpendicular anisotropy induced by the fcc-bcc structural transformation. [S0163-1829(97)00809-6]

I. INTRODUCTION

Magnetic ultrathin films represent model systems to study the unique magnetic properties due to reduced symmetry and dimension. In particular systems, for example, Fe/Cu(100),[1–3] Fe/Ag(100),[4–7] and Co/Au(111),[8,9] the broken symmetry at the surface and the interface gives rise to a large magnetocrystalline surface anisotropy E_{MSA}.[10] E_{MSA} may overcome the in-plane anisotropy in the low coverage range, leading to a perpendicular magnetization with respect to the film surface. The perpendicular magnetization is often associated with a magnetic instability due to various competing influences: the magnetization switches from the perpendicular to the in-plane direction, as the in-plane anisotropy compensates the perpendicular anisotropy at a higher coverage (above a critical thickness t_c). This phenomenon is referred to as spin-reorientation transition. In a simple picture, only two dominating terms, E_{MSA} and the shape anisotropy (E_{shape}) contribute to the anisotropy energy E (per unit volume) of the system. E describes the energy difference between normal and in-plane direction of magnetization with respect to the film surface:[10]

$$E=K_{\mathrm{eff}}\sin^2\theta=(2K_{\mathrm{MSA}}/t+K_{\mathrm{shape}})\sin^2\theta \qquad (1)$$

with

$$K_{\mathrm{shape}}=-\frac{1}{2}\mu_0 M_s .$$

Here, K_{eff} is the effective anisotropy (energy per unit volume) of the system, K_{MSA} (energy per unit area), and K_{shape} (energy per unit volume) denote the constants describing the surface and the shape anisotropy, respectively, θ is the angle between the magnetization direction and the film normal, M_s is the saturation magnetization, and $\mu_0=4\times10^{-7}$ $\mathrm{VsA^{-1}\,m^{-1}}$. The factor 2 takes contributions from two interfaces of the film into account, assuming both interfaces to be equal. According to Eq. (1), the critical thickness t_c for the spin reorientation transition, at which K_{eff} is equal to zero, is determined to be $-2K_{\mathrm{MSA}}/K_{\mathrm{shape}}$. The spin reorientation transition is thus due to the decreasing influence of K_{MSA} with film thickness. A sudden flip of the magnetization direction at t_c is expected. This simple approximation, however, is based on the following assumptions: First, the magnetization is uniform within the film. Second, there are no other anisotropy (e.g., strain-induced anisotropy) contribution besides K_{MSA} and K_{shape}. Third, higher order anisotropy terms are negligible. Fourth, K_{MSA} and K_{shape} are independent of film thickness. Nevertheless, if any change of the film structure upon varying thickness appears and affects anisotropies of the film, the spin reorientation transition can no longer be explained by the above approximation.

The role of higher order terms in the spin reorientation transition has been addressed by Fritzsche *et al.*:[11] the effective anisotropy K_{eff} of the system never vanishes totally due to the existence of higher order terms, often leading to a continuous transition from a perpendicular to an in-plane direction within a narrow coverage range rather than to a sudden spin flip. Such a narrow coverage range of 0.5–1 ML has been observed, for example, in hcp Co/Au(111) [8] as well as in Fe/Cu(100),[12,13] and the corresponding higher order (fourth order) terms have also been quantitatively determined for Fe(110) films on Cr(110) as well as for Pd-covered Co/Pd(111) films in Ref. 11. On the other hand, a change in crystalline structure may cause a more delicate influence on the critical thickness for the spin-reorientation transition than the effect of higher order anisotropy terms.

For the fcc-like Fe film this situation gives at least two interesting aspects regarding the correlation of magnetism and structure: one concerning the dependence of the magnetic phase (a long-range ordered magnetic state) on the crystalline structure (the lattice parameter); the other being the interplay between the spin-reorientation transition and an fcc-bcc structural transformation, which has to occur in Fe films. The first aspect has been widely investigated for the Fe/Cu(100) system, in which the magnetic phase was shown to be sensitive to the crystalline structure, depending on the thickness and growth conditions (see, e.g., Refs. 14, 15). An fct-fcc structural transformation in Fe/Cu(100) grown at room temperature (RT) is responsible for the transition from the ferromagnetic phase to an antiferromagnetic (or a paramagnetic) phase.[14,15] This is due to the dependence of the

magnetic phase on the lattice parameter.[16–19] The shape anisotropy of the system stems only from the ferromagnetically ordered top layers rather than from the whole film, and its contribution is independent of the film thickness. The spin reorientation transition in RT-grown Fe/Cu(100) occurs therefore at a much higher coverages than for films grown at low temperature (LT), in which only the ferromagnetic phase is found.[14] So far, this aspect is experimentally and theoretically reasonably understood. On the contrary, for the second aspect a deeper understanding is still lacking up to now. The spin-reorientation transition observed in Fe/Cu(100) films has been associated with a complicated structural transformation for both growth temperatures.[14,20] This implies that the physics of the spin-reorientation transition is far beyond the simple approximation of competing anisotropies mentioned above and its possible correlation with the structural transformation should be taken into account.

$Cu_3Au(100)$ has been choosen as an alternative substrate to clarify the dependence of the magnetic phase of fcc-like Fe on the lattice parameter mentioned above. According to theoretical predictions and experimental results fcc-like Fe reveals a ferromagnetic phase at a lattice constant of $a_0 = 3.64$ Å (from theory)[16] and an antiferromagnetic phase with $a_0 = 3.59$ Å (from bulk experiment).[17] The lattice constant $a_0 = 3.61$ Å of Cu lies midway between the values of the ferromagnetic and antiferromagnetic phases of fcc-Fe. This suggests an extreme sensitivity of the magnetic phase of Fe/Cu(100) on the crystallographic structure, which may be affected by different deposition conditions, such as the growth temperature. Cu_3Au has a larger lattice constant (3.75 Å), as compared to Cu, lying in the range of the ferromagnetic phase of fcc-like Fe. Arguing only on the basis of lattice parameter, one therefore expects that epitaxial Fe films on $Cu_3Au(100)$ should exhibit only the ferromagnetic phase, independent of the growth temperature. Furthermore, it is of general interest to achieve a deeper insight into how the magnetic anisotropies are modified by the crystalline structure and morphology in a magnetic thin film system. It is particularly important with the more stable magnetic phase expected in $Fe/Cu_3Au(100)$, to investigate in detail the possible influence of, for example, the structural transformation (fcc-like to bcc-like), and the surface or interface roughness on the spin-reorientation transition, and to identify the true origin for the spin-reorientation transition.

In this work we report on the spin-reorientation transition and structural transformation in $Fe/Cu_3Au(100)$ films. We address the study of the mechanisms leading to the spin-reorientation transition of fcc-like Fe films, based on results of structural and morphological studies and on magnetic data for different growth temperatures. In the $Fe/Cu_3Au(100)$ system, the spin-reorientation transition is shown to be correlated to an fcc-bcc structural transformation.

II. EXPERIMENTAL ASPECTS

All of our experiments were carried out *in situ* in UHV chambers. Since the apparatus, the properties of the alloy substrate $Cu_3Au(100)$ and the sample preparation have already been described elsewhere,[21] only a brief description of them will be given here.

The substrate for growing the Fe films was a (100) face of a disk-shaped Cu_3Au single crystal. Prior to deposition of the Fe films the $Cu_3Au(100)$ crystal was cleaned by 1.5 keV Ar^+ ion bombardment, annealed to 900 K for 2 min and finally tempered at 600 K for 30 min to restore the chemical ordering of the alloy substrate [$Cu_3Au(100)$ exhibits a chemical order/disorder transition at $\approx$ 660 K (Ref. 22)]. The degree of ordering was checked with low-energy electron diffraction and the diffraction pattern showed a clear and sharp $c(2\times2)$ superstructure after the final annealing procedure.

Fe films were deposited from an Fe wire of high purity (99.99%) heated by electron bombardment. After proper outgassing of the wire, mainly from nitrogen, the pressure during evaporation could be kept below 5×10^{-8} Pa at evaporation rates of several monolayers per min. Fe films were grown at two different temperatures, 300 K (referred to as RT growth) and 160 K (LT growth). The growth temperature was carefully controlled by cooling the manipulator with liquid nitrogen while reproducibly heating the sample up to the desired temperature within a range of $\pm$ 5 K. The deposition rate was $\approx$ 1 ML per min. After deposition at low temperature (LT growth) the films were briefly annealed at 300 K.

The magnetic properties of the films were studied by magneto-optical Kerr effect (MOKE), carried out *in situ* in a UHV chamber equipped with facilities for MOKE, Auger electron spectroscopy (AES) and low-energy electron diffraction (LEED). The AES system was mounted face-to-face with the LEED system, so that the diffracted electron beam could be displayed on the fluorescent screen. This permits a measurement of medium energy electron diffraction (MEED) by recording the specular beam intensity to monitor the growth of the films. The Fe thickness was determined by MEED and AES (see Ref. 21). For the MOKE measurements two He-Ne lasers with photoelastic modulators and one light detector were employed. The lasers and the detector are arranged in such a way that both the perpendicular and the in-plane Kerr signal can be measured by just rotating the sample around its vertical axis without any rearrangement of the optical elements. Such a arrangement allows a reliable measurement of the spin-reorientation transition, which needs a quasi-simultaneous uptake of both the perpendicular and the in-plane Kerr signal. LEED was used for the structural investigation of the films. As shown in Sec. III, the information on the crystalline structure was, based on a kinematic analysis, extracted from the LEED-$I(E)$ curves taken for the (00) diffraction beam. This method has been successfully employed for monitoring the vertical interlayer distance at a temperature variation in the Fe/Cu(100) system.[23]

The studies of the film morphology were carried out *in situ* in another UHV chamber equipped with scanning tunneling microscope (STM), AES, and iron evaporators. For RT growth the films could be deposited without removing the sample from the STM measurement position. With such a special design, the STM is able to follow the process of film growth in the very same region of the surface. For the series of STM measurements for LT growth, however, the sample was prepared at 160 K on a manipulator with a cooling system and transferred into the STM after deposition. All STM images were taken at room temperature in a constant current mode at a positive or negative sample bias voltage of $\approx$ 1.0 V and a tunneling current of $\approx$ 1.0 nA.

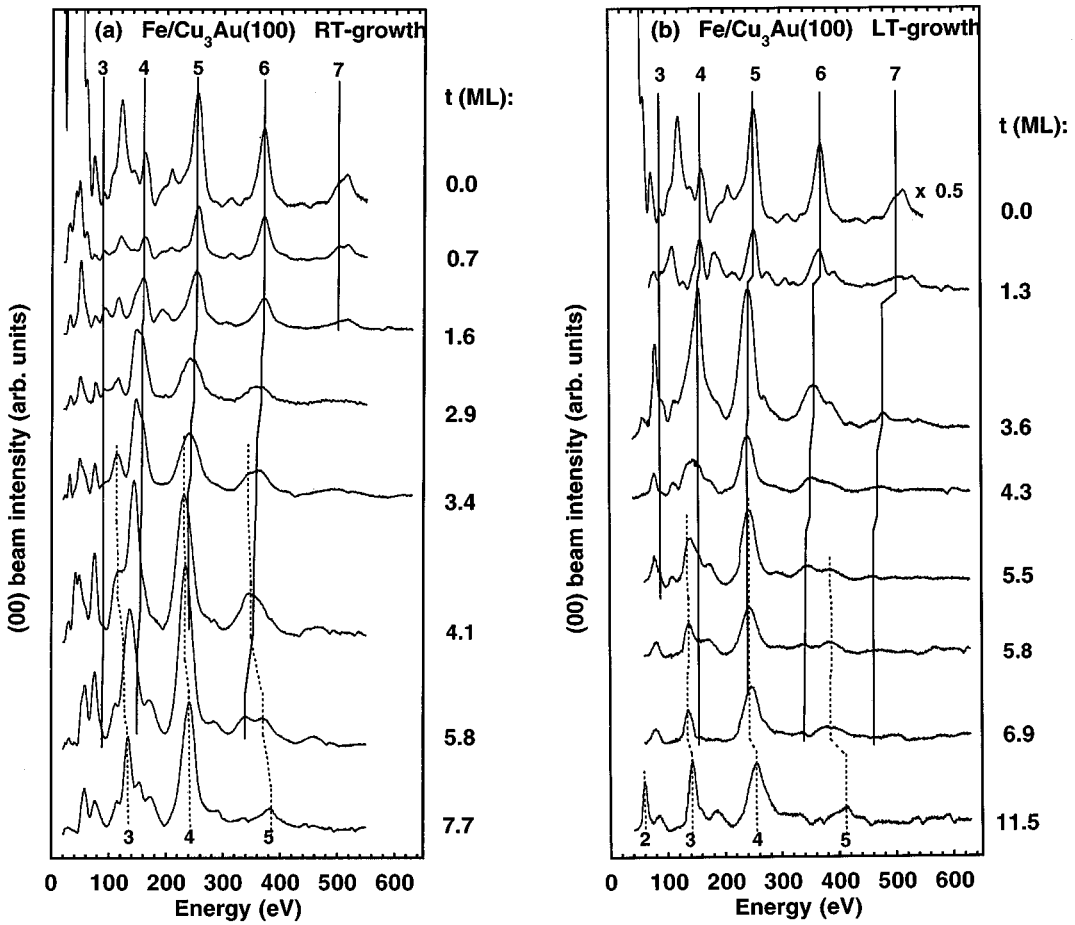

FIG. 1. (a): Intensity vs energy dependence of the LEED (00) beam for $Cu_3Au(100)$ and RT-grown $Fe/Cu_3Au(100)$ at various coverages. Two different periodic peak sequences with weight depending on the thickness are indicated by solid and dashed lines, respectively. The indices denoted are the integer numbers of the Bragg interference condition. (b): Same as (a), but for LT-grown $Fe/Cu_3Au(100)$ at various coverages.

Before we present the results of STM and LEED-$I(E)$ measurements, some particularities of the alloy substrate $Cu_3Au(100)$ should be briefly mentioned. Seen along the [100] direction of a well ordered Cu_3Au crystal there are two possible surface terminations: a pure Cu surface and a Au-rich surface with 50% gold concentration. A previous STM and low-energy ion scattering experiment indicated that the topmost layer of a well ordered $Cu_3Au(100)$ is only the Au-rich surface and correspondingly terraces should be separated by bilayer steps.[24] In order to get a good chemical order the authors of Ref. 24 performed an extensive annealing process of 10 h at 500 K. The analysis of the STM images of the $Cu_3Au(100)$ crystal used in this work shows, however, that both bilayer and monolayer steps were always present for the cases of up to 6 h annealing at 600 K. Moreover, there is no longer a distinct improvement of the chemical order and the surface configuration already after 30 min annealing at 600 K.[25] We thus have choosen 30 min annealing at 600 K as our preparation procedure prior to the Fe deposition.

III. fcc-bcc STRUCTURAL TRANSFORMATION IN $Fe/Cu_3Au(100)$

Figures 1(a)–1(b) reproduces the LEED-$I(E)$ curves of the (00) diffraction beam from $Fe/Cu_3Au(100)$ films for both growth temperatures. The LEED-$I(E)$ curves reveal two sequences of peak maxima with equal $\sqrt{E}$ distances, corresponding to two different structural phases. The numbers n indicate the integer count of the electron wavelengths fulfilling the condition of constructive interference, and are related to the vertical interlayer distance. The first peak sequence, marked by solid lines, is related to the fcc(100)-like phase in a pseudomorphic growth on the $Cu_3Au(100)$ substrate. Its intensity, however, decreases with increasing Fe thickness. The second peak sequence, marked by dotted lines, is seen in films of $\geqslant 3.4$ and $\geqslant 5.5$ ML for RT and LT growth, respectively. Its intensity increases with Fe thickness. Since some peaks in the LEED-$I(E)$ curves which are due to multiple scattering[26] may overlap the indicated peaks above, it is sometimes difficult to determine the exact onset of the second peak sequence (dotted lines). Our method is taking the ratio of the intensities of the second peak sequence (or the peak with the same energy position as one of the second peak sequence) to the first peak sequence (for example, the peak around 110 eV to the peak of the first sequence with index 4 in the case of RT growth and the peak around 380 eV to the peak of the first sequence with index 6 for LT growth). The onset thickness for the second structural phase is then such a thickness starting from which the ratio defined above increases with film thickness. The onset of the second peak sequence is thus carefully determined in this

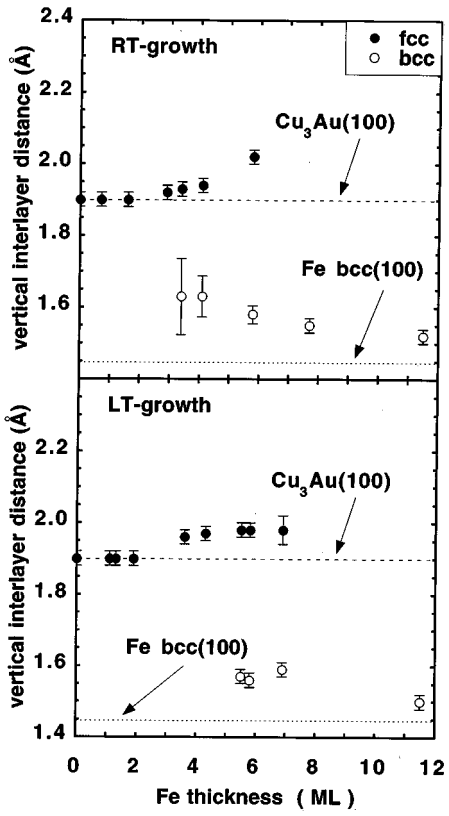

FIG. 2. Two different vertical interlayer distances $a_\perp$ calculated from the $I(E)$ curves of Fig. 1 are related to fcc-like (full circles) and bcc-like Fe (open circles), respectively. The values of the vertical interlayer distance of the $Cu_3Au(100)$ substrate and bcc(100)-Fe bulk are indicated by horizontal lines. Note that for both growth temperatures a superposition of the fcc- and bcc-like phases was found.

way to be at $\approx$ 3.5 ML for RT growth and $\approx$ 5.5 ML for LT growth. As shown later, this onset thickness obtained here agrees also well with the one extracted from STM images, at which one starts to observe the new structural phase (bcc-like) on the film surface.

Films at coverages of 3.4–5.8 ML for RT growth and 5.5–6.9 ML for LT growth are characterized by a coexistence of these two structural phases. At a coverage of 7.7 and 11.2 ML for RT and LT growth, respectively, the first peak sequence is almost invisible and only the second series can be observed.

The vertical interlayer distance $a_\perp$, corresponding to these two peak sequences, is extracted within the kinematic approximation, by using the following relation:[26]

$$a_\perp(n) = \frac{n\pi\hbar}{\sqrt{2m(E_p+V_0)}\sin\theta}. \qquad (2)$$

Here, E_p is the primary energy of the electron, V_0 the additional energy shift due to the average inner potential in the crystal, m electron mass, and θ the incident angle with respect to the sample surface. $a_\perp$ is finally determined by a linear regression of the plot $a_\perp(n)$.

In Figs. 2(a) and 2(b) $a_\perp$ is depicted as a function of the Fe thickness for both growth temperatures. For the clean substrate we obtain $a_\perp = (1.89 \pm 0.02)$ Å which is only slightly larger than the literature value of 1.875 Å.[27] In the case of RT growth [Fig. 2(a)], the value of $a_\perp$ from the first peak sequence does not change for films up to 2.0 ML, indicating a registry of the film with the substrate, i.e., an fcc-like continuation. At higher coverages (2.9–5.8 ML) $a_\perp$ increases with the film thickness. $a_\perp$ has a value of approximately 2.0 Å at 5.8 ML, but only with a very weak peak intensity. This indicates the disappearance of the fcc-like phase at high coverages within the limited probing depth of LEED ($\approx$2–3 ML), yet does not exclude the presence of an fcc-like structure in deeper layers.

As mentioned above, the second sequence starts at a coverage of $\approx$ 3.4 ML for RT growth. The corresponding value of $a_\perp$ is about 1.6 Å at coverages of 3.4 and 4.1 ML, then decreases with Fe thickness, reaching a value of approximately 1.5 Å at higher coverages of 7.7 and 11.5 ML [not shown in Fig. 1(a)]. As shown in Fig. 1(a), the corresponding energy peaks in the LEED-$I(E)$ curves become predominant with increasing thickness. All of the values of $a_\perp$ of the second peak sequence are close to the interlayer distance in (100) oriented bcc-like Fe ($a_\perp$ = 1.43 Å) rather than to that of a Fe bcc(110)-like structure ($a_\perp$ = 2.02 Å).

For LT growth $a_\perp$ is displayed in Fig. 2(b) as a function of thickness. Similar to the observation in RT-grown Fe/C $u_3Au(100)$, one finds two structural phases corresponding to two different interlayer distances. $a_\perp$ extracted from the first peak sequence has the same value for coverages up to $\approx$ 2 ML and increases with increasing thickness reaching a value of (1.98 ± 0.02) Å at 5.5 ML. The value of the corresponding $a_\perp$ of the second peak sequence, which becomes distinctly observable at a coverage of $\pm$ 5.5 ML, is (1.58 ± 0.02) Å. This value is again much smaller than the value for bcc(110)-like Fe (2.02 Å) and much closer to that of a bcc(100)-like Fe (1.43 Å). $a_\perp$ reaches a value of $\approx$ 1.50 Å at 11.5 ML. Moreover, the LEED patterns (not shown here) at these coverages show only a $p(1\times1)$ symmetry, different from those for bcc(110)-Fe found in Fe/Cu(100) (see, e.g., Refs. 14, 20, 28). This also implies that the second structural phase found at higher coverages has the low-index plane such as (100) orientated surface. Thus, we tend to conclude that for both growth temperatures, the fcc-like Fe transforms into a bcc-like phase with a (100) orientation, being different from the (110) orientation found in the Fe/Cu(100) system.[14,28]

The finding of an expanded vertical interlayer distance in the fcc-like region for both growth temperatures somehow contradicts to the usual assumption that, in pseudomorphic films with an expanded in-plane lattice, the perpendicular lattice parameter should be contracted. In order to keep the atomic volume constant within electrostatic models, this contraction is determined by the Poisson ratio.[29] This belief, however, becomes more questionable when taking the complicated correlation of the lattice parameter (or lattice distortion) and magnetic moment as well as the magnetic phase in fcc-like Fe into account. Various ferromagnetic metastable fct states, which are connected to different values of the lattice parameter or c/a, are possible.[30,31] Bulk calculations have shown that the magnetic moment increases with in-

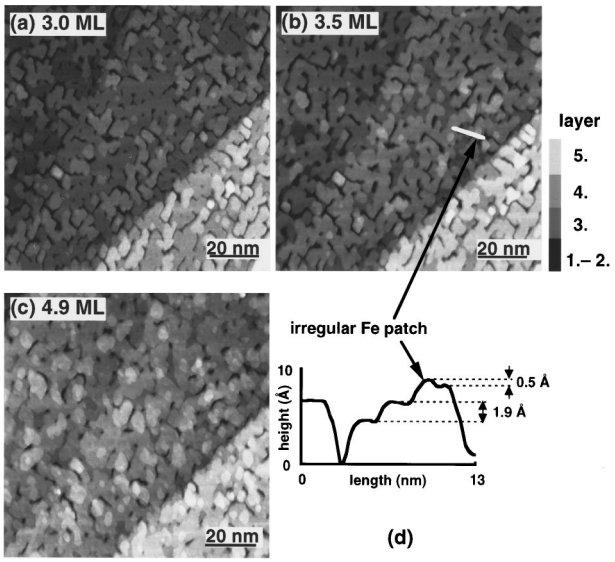

FIG. 3. STM images of (a) 3.0 ML, (b) 3.5 ML, and (c) 4.9 ML Fe films on $Cu_3Au(100)$ for RT growth; (d) the height profile plot along the line indicated in (b). The gray scale is used for the images (a) and (b) to indicate the corresponding layer on the middle terrace. Two values of step heights are shown in (d): 1.9 Å for the regular island and the irregular height of 0.5 Å.

creasing lattice constant.[16,18,30,32] By using site-specific Mössbauer spectroscopy, D. J. Keavney *et al.*[19] have observed that the average moment of fcc-like Fe films, which were deposited on $Cu_{1-x}Au_x(100)$ with varying lattice constant a_0, increases with a_0. Unfortunately these authors do not comment on whether or not the corresponding vertical interlayer distance in these films is contracted.

Another interesting finding is the coexistence of both fcc- and bcc-like structural peaks in the LEED-$I(E)$ spectra. Moreover, the intensity of the fcc(bcc)-related peak sequence decreases (increases) with film thickness. In order to obtain more detailed information on the behavior of the fcc-bcc transformation we performed STM measurements in this thickness range. Figures 3(a)–3(c) show the STM images for 3.0, 3.5, and 4.9 ML RT-grown $Fe/Cu_3Au(100)$, respectively. At a coverage of 3.0 ML, the first and second layer (the darkest part on each terrace) are almost completely filled (more than 95 and 90% layer filling for the first and second layer, respectively). What one can see in this image is mostly the surface of the third and the fourth layer (the second brightest and the brightest part in each terrace). The third layer is also nearly completed (82% layer filling). There are already many islands of the fourth layer with 31% layer filling. Note that the islands reveal a regular shape. The line scan gives a height of the Fe layer of (1.9 ± 0.2) Å (not shown here). This value corresponds to the vertical interlayer spacing of the substrate, indicating an fcc-like structure of the Fe layers.

On a thicker film of 3.5 ML [Fig. 3(b)] some small irregular patches on the topmost islands start to show up. The line scan profile in Fig. 3(d) shows two typical heights: (1.9 ± 0.2) and (0.5 ± 0.2) Å. The former corresponds to the height of fcc-like Fe layers, as observed at lower coverages. The latter indicates the presence of a certain distorted structure, possibly related to a dislocation or a buckling of the Fe

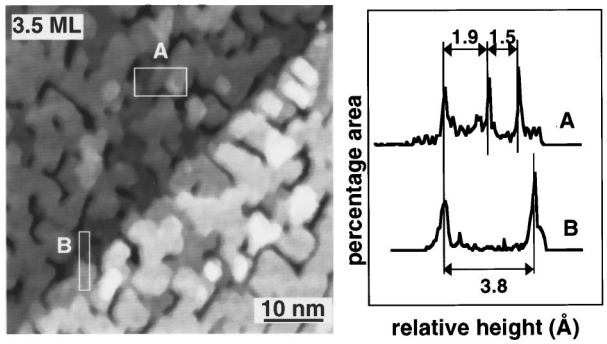

FIG. 4. Left: enlargement of Fig. 3(b) [3.5 ML RT-grown $Fe/Cu_3Au(100)$]. Right: height distributions of two areas denoted A and B, as indicated by white rectangles. Note that the line scan shown in Fig. 3(d) lies in the region indicated by A.

film. This fractional height of 0.5 Å makes it impossible to determine the crystallographic structure of the ''irregular'' Fe patches from a single line scan. Nevertheless, as will be shown in Figs. 4 and 5, by taking a histogram of the height distribution in the vicinity of these irregular Fe patches, one can obtain further structural information. It is legitimate, however, to infer that these irregular Fe patches are related to some kind of fcc-bcc transformation.

Increasing the Fe thickness further, the fractional height Fe patches become larger and more numerous and reveal more irregular shapes, in contrast to Fe islands at low coverages. On the 4.9 ML film Fig. 3(c), the irregular Fe patches dominate the surface so that the surface becomes rougher than that at 3–4 ML. Most of the regular islands are now covered by irregular Fe patches and only few of them remain visible in the STM image of 4.9 ML.

Measuring the height or the interlayer spacing of steps between Fe layers or islands from STM images, allows a determination of the structural phase of the topmost layer (fcc- or bcc-like). For this purpose, we take a histogram of the height distribution within a selected area and measure the distance between neighboring peaks in the histogram. Figure 4 shows the height distribution of two areas denoted A and B, as indicated by white rectangles in the STM image of 3.5 ML $Fe/Cu_3Au(100)$, which is a magnification of Fig. 3(b). The area A includes an irregular Fe patch (white gray) and regular Fe layers (gray and black). The histogram of the height distribution taken over the area A indicates two dif-

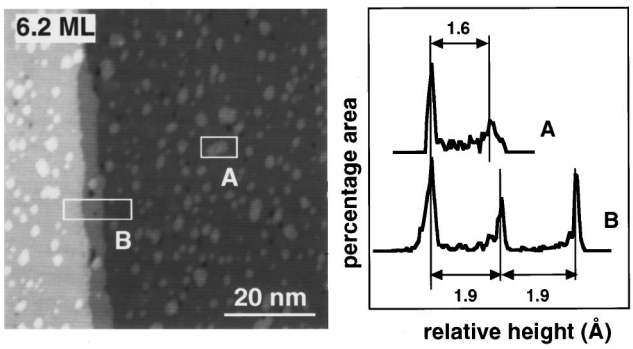

FIG. 5. STM image of LT-grown 6.2 ML $Fe/Cu_3Au(100)$ (left side) and height distributions (right side) of two areas denoted A and B, as indicated by white rectangles in the STM image.

ferent layer distances: 1.9 and 1.5 Å. The former is, as indicated in the line scan of Fig. 3(d), the value corresponding to the fcc-like layers. The latter can be identified with the interlayer distance of (100)-oriented bcc-like Fe. For comparison, area B is chosen across the edge of a bilayer step. The layer distance between the regular Fe layers located on the upper and the lower terrace is shown to be 3.8 Å, being consistent with the height of a bilayer step on the $Cu_3Au(100)$ surface. All the height distributions taken at higher coverages (4.0 and 4.9 ML) show the layer height of the irregular patches to be 1.5–1.6 Å. This confirms the speculation made above that the irregular Fe patches mark the onset of an fcc-bcc structural transformation, and indicates furthermore that the irregular Fe patches have a bcc-like structure with (100) orientation. Since the irregular patches are only found in Fe films thicker than 3.5 ML, it can be concluded that an fcc(100)-bcc(100) transition starts beginning at $\approx$ 3.5 ML with some small irregular patches (bcc-like Fe patches) on the topmost regular Fe layers (fcc-like Fe). These results agree very well with those obtained from our LEED-$I(E)$ curves. Moreover, with increasing film thickness, the irregular Fe layers become predominant at the film surface, as seen in the 4.9 ML Fe film [Fig. 3(c)]. Note that the fcc-like Fe layers which are not yet covered by bcc-like Fe layers still retain their regular island form and layer height, without any distinct indication of changes in morphology or structure. These results suggest that (i) the bcc-like Fe grows on the topmost fcc-like layers with increasing Fe thickness and (ii) the fcc-like underlayers seem to conserve their fcc-like structure at least up to a certain thickness.

For the case of LT growth, Fig. 5 shows the STM image of a 6.2 ML film and the height distribution of two selected areas. The film at 6.2 ML shows an astonishing surface morphology. The almost completely closed layer is the sixth layer, where only some opening to the lower layers can be seen. The bright spots are islands of the seventh layer. Despite its appearance in Fig. 5, the surface of the sixth layer is not as smooth as what is usually found in a good layer-by-layer growth. On a smaller scale (not shown here), we see a networklike fine structure with small nearly square meshes on the closed film, which may be attributed to some vertical buckling of atoms. The mismatch-strain in this almost-closed film could be accommodated by building up such a networklike fine structure. The reason for the appearance of this almost-closed film at LT growth and the origin of the networklike fine structure will be described in more detail in our forthcoming paper.[25] Here we will focus our attention on the aspect of the fcc-bcc structural transformation. The right-hand panel in Fig. 5 shows the height distribution taken on two different areas denoted A and B, and indicated by the white rectangles in the STM image at the left hand panel. At area B, a value of the interlayer height of 1.9 Å is obtained, which is consistent with the registry of the fcc structure on the substrate. The height distribution of area A gives an island height with respect to the almost closed layer of about 1.6 Å. This value is significantly out of registry with the Fe fcc(100)-like structure and consistent with the interlayer distance of the bcc-like phase of Fe oriented with the (100) plane parallel to the substrate surface. The islands are thus expected to be bcc-like phase. This finding agrees very well with the results of the LEED-$I(E)$ studies shown above.

Combining the findings of STM and LEED, one can conclude that—starting from a coverage of $\approx$ 3.5 ML for RT growth and $\approx$ 5.5 ML for LT growth—the bcc-like Fe patches with an irregular shape grow on top of the fcc-like islands (or layers) and progressively cover the surface of the as-grown fcc-like underlayers. Both LEED and STM data show that the bcc-like Fe has a (100) orientation, being different from the (110) orientation found in Fe/Cu(100). The coexistence of the fcc- and bcc-like phases in LEED data indicates that the as-grown fcc-like Fe underlayers or parts of them still retain their structure at least up to a higher coverage. The absence of an fcc-related peak sequence in LEED-$I(E)$ curves at higher coverages should thus be mainly attributed to the intensity attenuation of the diffracted electron beam through the bcc-like overlayers due to its small probing depth. A pronounced structural transformation proceeding in the fcc-like underlayers like the martensitic transformation found in RT-grown Fe/Cu(100)[33,34] seems not to take place in the present case.

IV. SPIN-REORIENTATION TRANSITION

Figure 6 compiles hysteresis loops of RT grown films on $Cu_3Au(100)$ taken at 160 K in both polar and longitudinal geometries for various Fe coverages. The shape of the hysteresis loops clearly reveals a strong dependence on the thickness. In the case of RT growth [Fig. 6(a)], the distinct ferromagnetic response is found only in films with coverages starting from 2.1 ML in the polar geometry. Below this coverage no ferromagnetic response is found, indicating the absence of a long-range ferromagnetic order at 160 K. The remanence at 2.1 ML is still very small, but already becomes more evident at a higher coverage of 2.2 ML. An almost rectangular loop is observed at higher coverages from 2.5 and 3 ML, indicating an easy direction of the magnetization perpendicular to the film plane and a clear presence of the perpendicular anisotropy. Above 3 ML the shape of loops reveals a pronounced change, developing a sheared ''hourglass'' shape up to about 3.5 ML. Since the in-plane component of the Kerr signal is still zero up to this coverages, this development of the loop shape would be related to the formation of domains rather than to a sizable rotation of the magnetization.[21] The spin-reorientation transition shows up at coverages above 3.5 ML with a strong reduction of the remanence in the perpendicular component and increase in the in-plane component. The polar magnetic response takes more and more the form of a hard axis loop, and pronounced rectangular loops in the in-plane component, starting from 3.8 ML, appear with increasing remanence signal and coercive field with coverage up to 7.3 ML.

The hysteresis loops of LT grown Fe films on $Cu_3Au(100)$ are shown in Fig. 6(b). Similar to those in the case of RT growth, the compilation shows also a strong variation of the hysteresis loops with coverage. Different from the case of RT growth, however, one finds a small ferromagnetic response in the polar geometry already at a coverage of 1.1 and 1.3 ML. At a coverage of 1.9 ML an almost rectangular loop with slightly rounded edges and inclined slope is observed. This hysteresis loop is characterized by a large remanence, indicating an easy axis of magnetization perpendicular to the film surface. Such a hysteresis loop

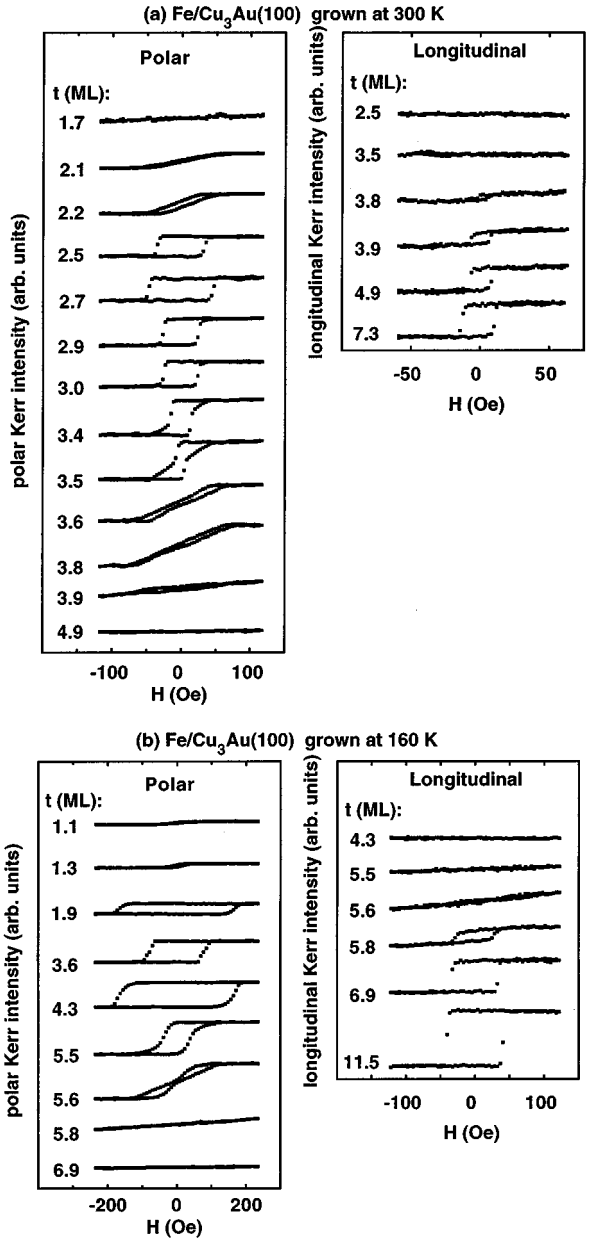

FIG. 6. Compilations of hysteresis loops in the polar (left panel) and longitudinal (right panel) Kerr effect for $Fe/Cu_3Au(100)$ of various coverages grown at (a) 300 K (RT) and (b) 160 K (LT), and annealed to 300 K. The measuring temperature is 160 K.

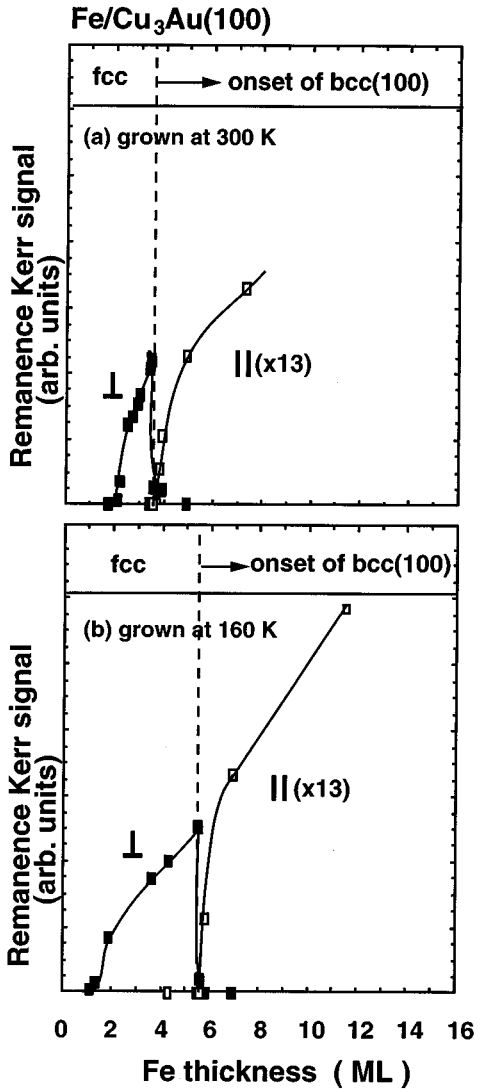

FIG. 7. Overview of the correlation of the spin-reorientation transition and the structural transformation in $Fe/Cu_3Au(100)$ for both growth temperatures. The magnetic parts show thickness dependence of the perpendicular (solid squares) and in-plane (open squares) remanence Kerr signal measured at 160 K. (Solid lines serve as a guide to the eye only.) The spin-reorientation transition is observed at about 3.5 and 5.5 ML for RT and LT growth, respectively. The dashed lines denote the onset of the growth of the bcc-like phase at the film surface, but the fcc-like underlayers maintain their structure at least up to a certain higher coverage. Note that the onset thickness of the fcc-bcc structural transformation coincides with the critical thickness for the spin-reorientation transition.

is found in all films with coverages between 1.9 and 5.5 ML. The hysteresis loop at a coverage of 5.5 ML reveals a large slope. At a coverage of 5.6 ML, the hysteresis loop undergoes a pronounced change, having a strongly sheared ''hourglass'' shape as found in RT-grown films. Films thicker than 5.6 ML show no perpendicular ferromagnetic response.

Parallel to the decrease of the perpendicular remanence at coverages between 5.5 and 5.8 ML for LT-grown films, the longitudinal Kerr signal indicates an onset of the in-plane remanence. The coercive field at 5.6 ML is still too high for the in-plane magnetization to be forced into the film surface, showing only a weak variation with the applied field. A rectangular loop is found at a coverage of 5.8 ML, corresponding to an in-plane easy axis of magnetization. Both the in-plane remanence Kerr signal and coercive field increase with the Fe thickness up to 11.5 ML. Similar to those findings in the case of RT growth, the system exhibits also a continuous change of the magnetization direction rather than a sudden flip at a certain coverage. Note that the onset coverage of the spin reorientation transition for the LT grown films has a larger value ($\approx$ 5.5 ML) than the one (only $\approx$ 3.5 ML) in the case of RT growth.

Figure 7 summarizes the results of the structural investigation, which has been shown in the last section, and the remanence Kerr signal extracted from hysteresis loops shown in Fig. 6 of $Fe/Cu_3Au(100)$ films in different thick-

ness regimes for both growth temperatures. We first concentrate our attention on the magnetic part of Fig. 7. Both the perpendicular and the in-plane remanence Kerr signals measured at 160 K are plotted as a function of the Fe thickness, giving a more quantitative information than the hysteresis loops in Fig. 6. From Fig. 7 the thickness range for the presence of a perpendicular remanence at 160 K is determined to be between 2.1 and 3.5 ML for RT growth and between 1.1 and 5.5 ML for LT growth. The perpendicular remanence Kerr signal increases linearly with the thickness from 2.5 to 3.5 ML and from 1.9 to 5.5 ML for RT and LT growth, respectively, indicating the presence of a ferromagnetic order in the whole film. This behavior is found in both RT and LT growth. As mentioned in the introduction, this is because $Cu_3Au(100)$ may—independent of the growth temperature—only stabilize ferromagnetic fcc-like Fe films due to its enhanced lattice constant. Our result agrees well with theoretical predictions.[16,18] Obviously $Cu_3Au(100)$ provides a more stable environment in the sense of the magnetic phase for the study of the relation of the fcc-bcc structural transformation and the spin-reorientation transition, as compared to the Fe/Cu(100) system.

Above 3.5 ML for RT and 5.5 ML for LT growth the perpendicular remanence Kerr signal decreases abruptly to zero within a narrow coverage range of $\approx$ 0.5 ML. At the same thickness the onset of an in-plane remanence Kerr signal is observed. This indicates a continuous spin-reorientation transition from a perpendicular to an in-plane direction. Accordingly, the critical thickness t_c for the spin reorientation transition at 160 K is found to be $\approx$ 3.5 and 5.5 ML for RT and LT growth, respectively. As indicated above, t_c strongly depends on the growth temperature. About 2 ML difference in t_c between RT- and LT-grown films is clearly visible by comparing Figs. 7(a) and 7(b).

V. DISCUSSION: CORRELATION OF SPIN REORIENTATION AND fcc-bcc STRUCTURAL TRANSFORMATION

In the following, based on our above experimental data, we will concentrate our discussion on the aspect of a correlation between the fcc-bcc structural and spin-reorientation transition. Figure 7 gives a overview of the relation between magnetism and structure for both RT and LT grown Fe/$Cu_3Au(100)$. We see immediately that for both growth temperatures the spin-reorientation transition coincides with the onset of the fcc-bcc structural transformation. As mentioned above, the critical thickness t_c for the spin-reorientation transition in Fe/$Cu_3Au(100)$ is around 3.5 and 5.5 ML for RT- and LT-growth, respectively. Films thinner than the critical thickness have a perpendicular easy axis and reveal an fcc-like structure. As shown by our STM and LEED investigations, the onset of an fcc(100)- bcc(100) structural transformation is found at the same thickness as the critical thickness t_c for the spin-reorientation transition. Based on this coincidence, one intuitively tends to correlate these two in both RT- and LT-grown films. Nevertheless, to achieve a deeper insight into the origins of this correlation, further considerations beyond a simple phenomenological comparison are still necessary. Thus, we discuss our findings from different physical points of view and arrange it as follows: In Sec. V A we consider the influence of the structural defects on the perpendicular anisotropy through the fcc-bcc structural transformation. The contribution of the growing bcc(100)-like Fe to the total anisotropy will also be discussed. Besides the effects, which are associated with the fcc-bcc structural transformation, we consider in Sec. V B the influence of strain, surface roughness, and interdiffusion in fcc-like Fe films on $Cu_3Au(100)$ on the magnetic anisotropy. In Sec. V C we examine the possibility for existence of a spin-reorientation-induced structural transformation, an approach opposite to that in Sec. V A.

A. Effects of the fcc-bcc structural transformation and the growing bcc(100)-like Fe on the perpendicular anisotropy

According to the MEED oscillations during the Fe evaporation[21] and the STM images shown above (or more details in Ref. 25), the as-grown bcc(100) Fe films on $Cu_3Au(100)$ are always accompanied by a relatively rough surface morphology. This morphology is connected to a large amount of dislocations and defects. As mentioned above, the magnetocrystalline surface anisotropy, which is assumed to be responsible for the existence of the perpendicular magnetization in Fe/$Cu_3Au(100)$ and Fe/Cu(100), is due to the broken symmetry of the crystalline structure at the surface and at the interface, and is consequently very sensitive to the quality of the film surface. A poor crystalline structure with dislocations and defects at the surface could obscure the symmetry character of the surface, and consequently may drastically reduce the magnetocrystalline surface anisotropy or the perpendicular anisotropy in our case, leading to a spin-reorientation transition. This effect is somewhat different from the one induced by the usual surface roughness, which will be shown below, according to the Bruno model[46,47] to be negligible in our case. The roughness effect in the Bruno model is mainly due to the different symmetry of atoms at step edges, i.e., due to one or several neighboring atoms, whereby the local crystalline structure is not affected. On the contrary, the existence of bcc-like Fe and the large amount of dislocations at the thickness range of the fcc-bcc structural transformation at the film surface not only enhances the surface roughness in the usual sense but also may drastically modify the crystalline structure and thus the electronic structure of the film surface. Such a pronounced change in the film surface quality can drastically reduce the magnetocrystalline surface anisotropy and lead to the spin-reorientation transition.

The magnetocrystalline surface anisotropy, however, is not the only source for the perpendicular magnetization in Fe/Cu(100) and Fe/$Cu_3Au(100)$. Recently, D. E. Fowler *et al.*[35] have reported for the Fe/Cu(100) system in a measurement of effective anisotropy field that, besides the magnetocrystalline surface anisotropy, a perpendicular volume anisotropy is found to have a crucial contribution to the perpendicular easy axis. This perpendicular volume anisotropy is assumed, according to Ref. 35, to be caused by the lattice distortion (expansion) normal to the film surface. As the Fe film transforms from fct to bcc phase, it is reduced to the value close to unstrained bulk bcc Fe. Nevertheless, an estimate of this perpendicular volume anisotropy within a mag-

netoelastic model gives a value one order of magnitude smaller than the measured one.[35] In the absence of a direct measurement of the magnetic anisotropy constant for $Fe/Cu_3Au(100)$, we cannot determine whether or not such a large perpendicular volume anisotropy also exists in our system. Even though, we can still conclude that both the magnetocrystalline surface anisotropy, as usually expected, and the large perpendicular volume anisotropy, as newly reported in Ref. 35, must be strongly modified by a pronounced change in crystalline structure and/or in strain as the fcc-bcc structural transformation occurs. A drastic reduction of the perpendicular anisotropy resulting from the structural transformation should therefore be the main link between the spin-reorientation transition and the fcc-bcc transformation in our system. Accordingly, the different critical thicknesses of the spin-reorientation transition may be mainly due to the different critical thicknesses for the fcc-bcc structural transformation, which are in turn affected by growth conditions such as the growth temperature. This is the first possible explanation for the correlation observed.

The next point to be discussed is the following: How may the growing bcc(100)-like Fe affect the total anisotropy of the film system besides the specific influence of dislocations and defects on the perpendicular anisotropy mentioned above? bcc-like Fe should have its own specific anisotropy contribution. Could it act as an in-plane anisotropy and be strong enough to cause the spin reorientation transition?

bcc(100)-like Fe has previously been stabilized on Ag(100) for RT growth[4,36] and revealed a perpendicular magnetization in a MOKE study at 200 K up to $\approx$ 6 ML due to a strong surface anisotropy.[5] In another study of LT-grown Fe/Ag(100) films by means of low-energy secondary electron spin polarization the system also shows a perpendicular magnetization (measured at 125 K) up to $\approx$ 6 ML.[13] This indicates that bcc(100)-like Fe on Ag(100) has a strong perpendicular anisotropy, which can support a perpendicular magnetization up to $\approx$ 6 ML against the shape anisotropy. According to this finding, the surface anisotropy of the bcc(100)-like Fe/vacuum interface may also contribute to the perpendicular anisotropy, and the intrinsic anisotropy contribution of a growing bcc(100)-like Fe may thus not be responsible for the spin reorientation transition and for the small value of the critical thickness in RT-grown $Fe/Cu_3Au(100)$ films. This is, however, not necessarily true if we take into account the magnetoelastic anisotropy due to misfit strain. Ag has a lattice constant of 4.09 Å and hence a nearest neighboring distance of 2.89 Å on the (100) plane, which matches closely with that of bcc(100) Fe (2.86 Å), giving a lattice mismatch of only 1%. The nearest-neighbor spacing for $Cu_3Au(100)$, however, is 2.65 Å, giving an enhanced lattice mismatch of 7.3% for bcc(100)-Fe. In a more detailed consideration,[25] the bcc(100)-like Fe films on $Cu_3Au(100)$ should reveal an incoherent growth, as many dislocations or defects are always found in bcc(100)-like Fe films on $Cu_3Au(100)$.[25] The strain (consequently the magnetoelastic anisotropy) in the thickness range of incoherent growth have been shown to be independent of the lattice mismatch, and to be relieved with $1/t$ (t is thickness) η.[37] This seemingly implies that the enhanced lattice mismatch between bcc(100) Fe and the $Cu_3Au(100)$ substrate is not responsible for a possibly reduced perpendicular anisotropy. Nevertheless, in a recent study of ultrathin Co films on $W(110)$, Fritzsche *et al.*[38] have reported that an additional constant (volume-type) strain term in the thickness range of incoherent growth is superimposed on the leading $1/t$ contribution. This volume-type strain is given by the strain $\varepsilon(=-\eta)$ in the coherent growth with a certain prefactor, depending therefore on the lattice mismatch. This leads to a dependence of the strain-induced anisotropy on the lattice mismatch even in the thickness range of incoherent growth. This residual volume-type strain contribution is, as suggested by the authors in Ref. 38, attributed to an energy barrier against the formation of mismatch dislocations, possibly as a typical consequence of the film being an artificial nonequilibrium state,[39] which is neglected in the Bruno approach in Ref. 40. This finding implies that the strain-induced anisotropy due to the mismatch of bcc-like Fe on $Cu_3Au(100)$ may be still larger than the one in Fe/Ag(100). Furthermore, surface magnetoelastic coupling coefficients B^s which were recently reported by O'Handley and co-workers[41–43] and by du Trémolet de Lacheisserie, [44] give also an additional magnetoelastic strain contribution to the magnetic surface anisotropy. Based on the above discussion, though in the absence of a characterization of strain [e.g., using HR-LEED (Ref. 45)], the bcc(100)-like Fe found on $Cu_3Au(100)$ is certainly a more complicated case than bcc(100)-like Fe on Ag(100). Instead of the perpendicular anisotropy found in Fe/Ag(100), the appearance of bcc(100)-like Fe in the $Fe/Cu_3Au(100)$ system may thus also provide an in-plane anisotropy or at least a reduced perpendicular anisotropy.

So far, the discussion about the origin of the spin-reorientation transition in $Fe/Cu_3Au(100)$ followed the idea of a structural transformation-induced mechanism: The switching of the easy axis of magnetization is attributed to a structural transformation [fcc(100)-like to bcc(100)-like in our case], which leads to a drastic change in the magnetic anisotropy. According to this idea, the effect of the growing bcc(100)-like Fe on the magnetic anisotropy, as discussed above, is responsible for the spin reorientation transition, rather than the intrinsic magnetic properties of the whole film. Nevertheless, besides the structural transformation-induced effect, the intrinsic magnetic properties, in general, may also influence the behavior of the spin-reorientation transition. For this reason, we will consider in the next subsection some possible intrinsic mechanisms of the spin-reorientation transition in $Fe/Cu_3Au(100)$ to see if they play a crucial role in our case.

B. Influence of strain, surface roughness, and interdiffusion in fcc-like $Fe/Cu_3Au(100)$

The critical thickness of the RT-grown $Fe/Cu_3Au(100)$ is, as shown above, 3.5 ML and much smaller than that for LT growth (5.5 ML). A reduction of the critical thickness in the context of the intrinsic magnetic properties can have various reasons. The first one is the magnetoelastic anisotropy of the fcc-like Fe films on $Cu_3Au(100)$ due to the enhanced strain because of the 4.2% mismatch. The magnetoelastic anisotropy may act as an additional in-plane anisotropy besides the shape anisotropy and tends to reduce the critical thickness. Nevertheless, since both RT- and LT-grown $Fe/Cu_3Au(100)$ films should have the same lattice mismatch,

the difference in the critical thickness between both films cannot be easily attributed to a magnetoelastic effect. Furthermore, the critical thickness of LT-grown Fe/Cu(100) (Ref. 1), was found to be the same as that of LT-grown Fe/C u_3Au(100). This suggests a mismatch-independent intrinsic magnetism on both substrates in the case of LT-grown Fe films. To clarify this ambiguity a systematic investigation of the strain as a function of thickness of Fe films on C u_3Au(100) at different growth temperatures accompanied by a comparative study of Fe/Cu(100) still needs to be done.

Other possible sources for affecting magnetic anisotropies are the effect of surface roughness and/or interdiffusion on the magnetocrystalline anisotropy. The influence of the surface roughness has been theoretically studied by Bruno, both for the dipolar anisotropy[46] and for the magnetocrystalline surface anisotropy.[47] According to the Bruno model, a rough surface is characterized by two geometrical parameters which can be extracted from STM data: One is the quantity called roughness σ, being defined as the mean square deviation from the plane with the averaged thickness, i.e., the experimentally measured surface topography. σ describes the height deviation from an ideally flat surface with the average height. The other quantity is the average lateral size ξ of flat islands on the surface. In the analysis of Bruno, the role of the island shape was assumed to be negligible and the surface was chosen to be composed of square terraces and craters of equal height σ and lateral size ξ.

Analogously to the in-plane shape anisotropy contribution due to the dipolar interaction, three-dimensional islands induce a magnetostatic anisotropy. When the magnetization is normal to the film surface, the magnetic charges appearing at the edge of islands give rise to an extra dipolar anisotropy along the direction normal to the surface plane, contributing to the perpendicular anisotropy. In contrast to the regular shape anisotropy (demagnetizing field), which is proportional to the volume, the roughness induced magnetic dipolar anisotropy is proportional to the surface area. According to the calculation of the magnetostatic energy by Bruno,[46] this additional dipolar surface anisotropy can be written as

$$K_{\mathrm{d}} = 2S2\pi M^2\left(\frac{3}{4}\right)\sigma \cdot f(\sigma/\xi)\sin^2\theta, \tag{3}$$

where S is the film area and the function f is a characteristic function of σ and ξ with values from 0 to 1. As an example, we extract $\sigma = 1.6$ Å and $\xi = 20$ Å from the STM data taken on 3.5 ML RT-grown Fe/Cu_3Au(100) of Fig. 3(b). This gives a value of K_{d} of the order of magnitude of 0.1 erg/cm^2. In comparison to the surface anisotropy, which has been estimated to be $\approx$ 1.4 erg/cm^2,[21] this roughness induced dipolar surface anisotropy is about one order of magnitude smaller. Accordingly, the influence of this dipolar surface anisotropy on the value of the critical thickness, which is determined by the compensation between perpendicular and in-plane anisotropy [see Eq. (1)], increases t_c by 10% only. This is too small as compared to the observed difference (2 ML) in t_c between RT and LT growth.

The second effect of the surface roughness is a reduction of the magnetocrystalline surface anisotropy. This effect has been studied within Néel's model.[47] According to the Néel model, the surface anisotropy is attributed to the asymmetric environment of the surface atoms as compared to bulk lattice sites. At rough surfaces the asymmetric character should be modified to a certain extent. As the in-plane neighbors are lacking, for the atoms which are located at the step edge, a modification of the asymmetry character and consequently a reduction of the magnetocrystalline surface anisotropy should be expected. Based on the symmetry argument, the reduction of the magnetocrystalline surface anisotropy $\Delta K^s_{\mathrm{cryst}}/K^s_{\mathrm{cryst}}$ is given as follows:[47]

$$\frac{\Delta K^s_{\mathrm{cryst}}}{K^s_{\mathrm{cryst}}} = -\frac{2\sigma}{\xi}, \tag{4}$$

where the σ and the ξ are the same characteristic parameters for the rough surface defined above. Taking the same values of σ and ξ for 3.5 ML RT-grown Fe film on Cu_3Au(100) as above, one gets a reduction of the magnetocrystalline surface anisotropy by less than 20% as compared to the one of the flat surface. A reduction of the magnetocrystalline anisotropy should lead to a smaller value of the critical thickness. According to Eq. (1), we can estimate the value of the critical thickness to be 20% smaller, giving only a difference of less than 1 ML in the critical thickness by taking the value of the critical thickness for LT-grown Fe/Cu_3Au(100) (5.5 ML). This value is substantially smaller than the 2 ML difference in the critical thickness between RT- and LT-grown Fe/Cu_3Au(100). Furthermore, comparing RT- and LT-grown Fe/Cu_3Au(100), one finds little difference regarding the value of the surface roughness. The surface roughness induced difference in the critical thickness of the RT- and LT-grown film is estimated to be only about 0.1 ML. Therefore, the pronounced difference in the critical thickness between RT- and LT-grown Fe/Cu_3Au(100) cannot be explained within the Bruno model by the effect of the surface roughness on the magnetic anisotropy. We thus exclude the surface roughness to be a relevant factor to affect t_c in our case.

Based on the consideration of the low surface free energy of Cu and Au with respect to Fe,[27] an interdiffusion at the interface or a surface segregation of substrate atoms onto the film surface has to be expected. In the system Fe/Au(100), recent investigations revealed that the Fe/Au interface is subject to a roughening process.[48–50] Our STM and Auger data at the initial stage of growth, however, did not show any evidence of interdiffusion and surface segregation of substrate atoms (details see Ref. 25). Interdiffusion and surface segregation seem to be very sensitive to the growth temperature and could be suppressed below a certain temperature. For completeness, it is still valuable to discuss the effect of interdiffusion or surface segregation on the magnetic anisotropy. The effect of mixing at the interface has been reported by Draaisma, Broeder, and Jonge.[51] In a pair-interaction model they showed that the interface anisotropy is very sensitive to the interdiffusion at interfaces. A 50% mixing between the adatoms and atoms of the substrate at the interface may lead to a 50% reduction of the interface anisotropy. The influence of a nonmagnetic coverage (or underlayer) on the magnetic anisotropy of the magnetic thin films (or sandwiches) has been also investigated by some groups.[52–57] A drastic increase of the perpendicular anisotropy in

X/Co/Au(111) with overlayer X=Au, Cu, or Pd has been found and is strongly peaked near 1 ML overlayer thickness.[52,54] Recently, a similar finding has also been shown for Co/Au(111) films with a Au wedge overlayer by using scanning electron microscopy with polarization analysis.[57] According to these results, a limited submonolayer coverage of Au on top of the magnetic layer should shift the critical thickness for the spin reorientation transition to higher coverages. If a similar mechanism also works in the Fe/Cu_3Au(100) system, the reduced critical thickness for RT-grown Fe/Cu_3Au(100) seems to contradict this finding, even when some Au atoms indeed segregate onto the film surface. Nevertheless, as described by Beauvillain *et al.* in Ref. 54, the influence of the overlayer on the interface anisotropy can be interpreted in terms of electronic effects due to band hybridization at the interface. It is thus possible that, other than in the X/Co/Au(111) system, the influence of a Au overlayer on the magnetic anisotropy in the Fe/Cu_3Au(100) system is reversed due to different details in band hybridization at the interface. To verify this point, further measurements similar to that in Refs. 52, 54 still need to be done.

C. Is a kind of spin-reorientation-induced structural transformation possible?

The above discussion may provide approaches in two opposite directions to explain the correlation of the spin-reorientation transition and the structural transformation. The first one concerns a structural transformation-induced spin-reorientation, which has been discussed in detail above. The second one considers their correlation in a totally opposite point of view: Is it possible that the spin-reorientation transition drives the fcc(100)-bcc(100) structural transformation observed in RT- and LT-grown Fe/Cu_3Au(100), thus becoming a spin-reorientation-induced structural transformation? As is well known, the fcc-bcc transformation in Fe films can spontaneously occur on the basis of thermodynamic arguments.[34] Nevertheless, such a structural instability may be also supported by a magnetostrictive effect,[58] leading to the occurrence of the structural transformation already at lower coverages. A change of the direction of the magnetization may give rise to a change in the sample length.[59,60] One of the usual cases is the fractional longitudinal change of length in the direction of the magnetization (called as the longitudinal magnetostriction). The longitudinal expansion there is accompanied by a transverse contraction, resulting only in a very small change in total volume in comparison. In connection with this point, we recall that the Bain path,[61] which is a kind of lattice deformation through a uniaxial contraction in the direction normal to the film surface and a biaxial expansion in the in-plane direction, is assumed to be the transformation path for the fcc-bcc structural transformation in Fe/Cu_3Au(100) films.[25] With the magnetization perpendicular to the iron film surface, according to the longitudinal magnetostriction, the Fe film tends to expand in the direction normal to the film surface and to contract in the in-plane direction, acting, thus, as the force against the Bain transformation. Switching the direction of the magnetization into the in-plane direction, the magnetostriction induces an in-plane expansion and a perpendicular contraction. This additional strain induced by the magnetostriction normal to the surface may thus drive the Bain transformation, resulting in the fcc-bcc structural transformation. This interpretation implies that the structural transformation in Fe/Cu_3Au(100) is induced by the spin reorientation transition and the spin reorientation transition itself is, in contrast to the first interpretation above, attributed to the intrinsic magnetic properties of the Fe film. Up to now, there is, to our knowledge, no quantitative information about the strain energy available which is necessary to drive the Bain transformation in an Fe ultrathin film system. Although a measurement of magnetostrictive constants for the Fe film is not available, the literature shows, however, only a negligible value of the magnetostriction ($\delta l/l$) (δl is the change in length l) of iron bulk, for example, along the $\langle 100 \rangle$ magnetization to be only in the order of magnitude of 10^{-5}–10^{-6}.[62] This seems to be too small for a strain necessary to induce the Bain path. In this crude estimate, a spin-reorientation transition-induced structural transformation should be unlikely. On the contrary, in the first approach (Sec. V A), the reduction of the perpendicular anisotropy due to the fcc-bcc structural transformation has led to a very plausible explanation for the correlation between the spin reorientation and the fcc-bcc structural transformation.

VI. SUMMARY

In contrast to Fe/Cu(100), we observe only ferromagnetic order in both RT- and LT-grown Fe films on Cu_3Au(100). The critical thickness for the spin reorientation transition is found to be about 3.5 and 5.5 ML for RT and LT growth, respectively. Around the critical thickness we found distinct changes in the surface topology associated with an onset of the structural transformation from an fcc-like to a bcc-like phase. Instead of a bcc(110)-like phase, as found in the Fe/Cu(100) system,[14] bcc-like Fe films on Cu_3Au(100) reveal a (100) orientation. Different from the martensitic transformation in RT-grown Fe/Cu(100),[33,34] where the fcc-bcc transition changes not only the surface topology but also the structure of all accumulated layers, the Fe layers on Cu_3Au(100), which are covered by growing bcc-like Fe, seem to retain their fcc-like structure at least up to a certain higher coverage.

The spin-reorientation transition of Fe/Cu_3Au(100) is shown to be correlated to the fcc-bcc structural transformation in films. It may be mainly attributed to the drastic reduction of the perpendicular anisotropy due to the fcc-bcc structural transformation. The effect of roughness is within the Bruno model shown to be negligible. We cannot, however, exclude the influence of the strain-induced anisotropy on the spin-reorientation transition. Characterization of the strain of fcc-like as well as bcc-like Fe layer in this system is thus reserved for a further separation of the different anisotropy contributions, which is necessary for clarifying the nature of correlation of the structural transformation and the spin-reorientation transition.

ACKNOWLEDGMENTS

We would like to thank Dr. J. Giergiel for valuable discussion and B. Zada and F. Pabisch for their expert technical support. This work was supported by the Deutsche Forschungsgemeinschaft under Grant No. Schn353/3.

*Author to whom correspondence should be addressed.

[1] D. Li, M. Freitag, J. Pearson, Z. Q. Qiu, and S. D. Bader, Phys. Rev. Lett. **72**, 3112 (1994).
[2] J. Thomassen, F. May, B. Feldmann, M. Wuttig, and H. Ibach, Phys. Rev. Lett. **69**, 3831 (1992).
[3] D. P. Pappas, K.-P. Kämper, and H. Hopster, Phys. Rev. Lett. **64**, 3179 (1990).
[4] B. Heinrich, K. B. Urquhart, J. R. Dutcher, S. T. Purcell, J. F. Cochran, A. S. Arrot, D. A. Steigerwald, and W. F. Egelhoff, Jr., J. Appl. Phys. **63**, 3863 (1988).
[5] Z. Q. Qiu, J. Pearson, and S. D. Bader, Phys. Rev. Lett. **70**, 1006 (1993).
[6] J. A. C. Bland, A. D. Johnson, R. D. Bateson, and H. J. Lauter, J. Magn. Magn. Mater. **104-107**, 1798 (1992).
[7] N. C. Koon, B. T. Jonker, F. A. Volkening, J. J. Krebs, and G. A. Prinz, Phys. Rev. Lett. **59**, 2463 (1987).
[8] R. Allenspach, M. Stampanoni, and A. Bischof, Phys. Rev. Lett. **65**, 3344 (1990).
[9] J. Pommier, P. Meyer, G. Pénissard, J. Ferré, P. Bruno, and D. Renard, Phys. Rev. Lett. **65**, 2054 (1990).
[10] *Ultrathin Magnetic Structures*, edited by J. A. C. Bland and B. Heinrich (Springer-Verlag, Berlin, 1994), Vol. 1.
[11] H. Fritzsche, J. Kohlhepp, H. J. Elmers, and U. Gradmann, Phys. Rev. B **49**, 15 665 (1994).
[12] R. Allenspach and A. Bischof, Phys. Rev. Lett. **69**, 3385 (1992).
[13] D. P. Pappas, C. R. Brundle, and H. Hopster, Phys. Rev. B **45**, 8169 (1992).
[14] S. Müller, P. Bayer, C. Reischl, K. Heinz, B. Feldmann, H. Zillgen, and M. Wuttig, Phys. Rev. Lett. **74**, 765 (1995).
[15] R. D. Ellerbrock, A. Fuest, A. Schatz, W. Keune, and R. A. Brand, Phys. Rev. Lett. **74**, 3053 (1995).
[16] G. L. Krasko and G. B. Olson, J. Appl. Phys. **67**, 4570 (1990).
[17] S. H. Lu, J. Quinn, D. Tian, F. Jona, and P. M. Marcus, Surf. Sci. **209**, 364 (1989).
[18] V. L. Moruzzi, P. M. Marcus, K. Schwarz, and P. Mohn, Phys. Rev. B **34**, 1784 (1986).
[19] D. J. Keavney, D. F. Storm, J. W. Freeland, I. L. Grigorov, and J. C. Walker, Phys. Rev. Lett. **74**, 4531 (1995).
[20] S. Müller, P. Bayer, A. Kinne, C. Reischl, R. Metzler, and K. Heinz, Surf. Sci. **331-333**, 723 (1995).
[21] F. Baudelet, M.-T. Lin, W. Kuch, K. Meinel, B. Choi, C. M. Schneider, and J. Kirschner, Phys. Rev. B **51**, 12 563 (1995).
[22] R. Smoluchowski, in, *Hand Book of Physics*, edited by E. U. Condon *et al.* (McGraw-Hill, New York, 1967), pp. 8–97.
[23] M. Zharnikov, A. Dittschar, W. Kuch, C. M. Schneider, and J. Kirschner, Phys. Rev. Lett. **76**, 4620 (1996).
[24] H. Niehus and C. Achete, Surf. Sci. **289**, 19 (1993).
[25] M.-T. Lin, J. Shen, J. Giergiel, W. Kuch, H. Jenniches, M. Klaua, C. M. Schneider, and J. Kirschner (unpublished).
[26] J. B. Pendry, *Low Energy Electron Diffraction* (Academic, New York, 1974).
[27] W. B. Pearson, *A Handbook of Lattice Spacings and Structures of Metals and Alloys* (Pergamon, New York, 1967).
[28] P. Schmailzl, K. Schmidt, P. Bayer, R. Doell, and K. Heinz, Surf. Sci. **312**, 73-81 (1994).
[29] P. Jiang, P. M. Marcus, and F. Jona, Solid State Commun. **59**, 275 (1986).
[30] G. L. Krasko and G. B. Olson, Phys. Rev. B **40**, 11 536 (1989).
[31] Note, however, that they are unstable with respect to tetragonal deformation and would transform into the stable ferromagnetic bcc phase, which has the lowest energy (see Ref. 30).
[32] V. L. Moruzzi, P. M. Marcus, and J. Kübler, Phys. Rev. B **39**, 6957 (1989).
[33] K. Kalki, D. D. Chambliss, K. E. Johnson, R. J. Wilson, and S. Chiang, Phys. Rev. B **48**, 18 344 (1993).
[34] J. Giergiel, J. Kirschner, J. Landgraf, J. Shen, and J. Woltersdorf, Surf. Sci. **310**, 1 (1994).
[35] D. E. Fowler and J. V. Barth, Phys. Rev. B **53**, 5563 (1996).
[36] B. T. Jonker, K. H. Walker, E. Kisker, G. A. Prinz, and C. Carbone, Phys. Rev. Lett. **57**, 142 (1986).
[37] P. Bruno and J.-P. Renard, App. Phys. A **49**, 499 (1989).
[38] H. Fritzsche, J. Kohlhepp, and U. Gradmann, Phys. Rev. B **51**, 15 933 (1995).
[39] K.-N. Tu, J. W. Mayer, and L. C. Feldman, *Electronic Thin Film Science* (Macmillan, New York, 1992).
[40] C. Chappert and P. Bruno, J. Appl. Phys. **64**, 5736 (1988).
[41] S. W. Sun and R. C. O'Handley, Phys. Rev. Lett. **66**, 2798 (1991).
[42] G. Bochi, O. Song, and R. C. O'Handley, Phys. Rev. B **50**, 2043 (1994).
[43] O. Song, C. A. Ballentine, and R. C. O'Handley, Appl. Phys. Lett. **64**, 2593 (1994).
[44] E. du Trémolet de Lacheisserie, Phys. Rev. B **51**, 15 925 (1995).
[45] U. Scheithauer, G. Meyer, and M. Henzler, Surf. Sci. **178**, 441 (1986).
[46] P. Bruno, J. Appl. Phys. **64**, 3153 (1988).
[47] P. Bruno, J. Phys. F **18**, 1291 (1988).
[48] Y.-L. He and G.-C. Wang, Phys. Rev. Lett. **71**, 3834 (1993).
[49] Q. Jiang, Y.-L. He, and G.-C. Wang, Surf. Sci. **295**, 197 (1993).
[50] A. M. Begley, S. K. Kim, J. Quinn, H. Over, and P. M. Marcus, Phys. Rev. B **48**, 1779 (1993).
[51] H. J. G. Draaisma, F. J. A. d. Broeder, and W. J. M. d. Jonge, J. Appl. Phys. **63**, 3479 (1988).
[52] B. N. Engel, M. H. Wiedmann, R. A. Van Leeuwen, and C. M. Falco, Phys. Rev. B **48**, 9894 (1993).
[53] B. N. Engel, M. H. Wiedmann, R. A. Van Leeuwen, and C. M. Falco, J. Appl. Phys. **73**, 6192 (1993).
[54] P. Beauvillain, A. Bounouh, C. Chappert, R. Mégy, S. Ould-Mahfoud, J. P. Renard, P. Veillet, D. Weller, and J. Corno, J. Appl. Phys. **76**, 6078 (1994).
[55] F. O. Schumann, M. E. Buckley, and J. A. C. Bland, J. Appl. Phys. **76**, 6093 (1994).
[56] B. N. Engel, C. Marliére, and C. M. Falco, IEEE Trans. Magn. (to be published).
[57] W. Lutzke, M. Speckmann, and H. P. Oepen (unpublished).
[58] S. Chikazumi and S. H. Charap, *Physics of Magnetism* (Wiley, New York, 1964).
[59] E. W. Lee, Rep. Prog. Phys. **18**, 184 (1955).
[60] R. R. Birss, Adv. Phys. **8**, 252 (1959).
[61] E. C. Bain, Trans. AIME **70**, 25 (1924).
[62] E. Kneller, *Ferromagnetism* (Springer, Berlin, 1962).